Atmos. Chem. Phys. Discuss., 10, 22109–22130, 2010
www.atmos-chem-phys-discuss.net/10/22109/2010/
doi:10.5194/acpd-10-22109-2010

Atmospheric
Chemistry
and Physics
Discussions

A global survey of aerosol-liquid water cloud overlap based on four years of CALIPSO-CALIOP data

A. Devasthale[1] **and M. A. Thomas**[2]

[1]Remote Sensing Division, Swedish Meteorological and Hydrological Institute, Norrköping, Sweden
[2]Air Quality Division, Swedish Meteorological and Hydrological Institute, Norrköping, Sweden

Received: 13 August 2010 – Accepted: 20 September 2010 – Published: 27 September 2010

Correspondence to: A. Devasthale (abhay.devasthale@smhi.se)

Published by Copernicus Publications on behalf of the European Geosciences Union.

Abstract

The presence of aerosols over highly reflective liquid water cloud tops poses a big challenge in simulating their radiative impacts. Particularly, absorbing aerosols, such as smoke, may have significant impact in such situations and even change the sign of net radiative forcing. Until now, it was not possible to obtain information on such overlap events realistically from the existing passive satellite sensors. However, the CALIOP instrument onboard NASA's CALIPSO satellite allows us to examine these events with an unprecedented accuracy.

Using four years of collocated CALIPSO 5 km Aerosol and Cloud Layer Version 3 Products (June 2006–May 2010), we quantify, for the first time, the macrophysical characteristics of overlapping aerosol and water cloud layers globally. We investigate seasonal variability in these characteristics over six latitude bands to understand the hemispheric differences. We compute a) the percentage cases when such overlap is seen globally and seasonally when all aerosol types are included (AAO case) in the analysis, b) the joint histograms of aerosol layer base height and cloud layer top height, and c) the joint histograms of aerosol and cloud geometrical thicknesses in such overlap cases. We also investigate frequency of smoke aerosol-cloud overlap (SAO case).

The results show a distinct seasonality in overlap frequency in both AAO and SAO cases. Globally, the frequency is highest during JJA months in AAO case, while for the SAO case, it is highest in SON months. The seasonal mean overlap frequency can regionally exceed 20% in AAO case and 10% in SAO case. There is a tendency that the vertical separation between aerosol and cloud layers increases from high to low latitude regions in the both hemispheres. In about 5–10% cases the vertical distance between aerosol and cloud layers is less than 100 m, while about in 45–60% cases it less than a kilometer in the annual means for different latitudinal bands. The frequency of occurrence of thicker aerosol layers gradually increases from poles to tropics. In about 70–80% cases, aerosol layers are less than a kilometer thick, while in about 18–22% cases they are 1–2 km thick. The frequency of aerosol layers 2–3 km thick is about 4–5% in the tropical belts during overlap events. The results further highlight spatial and temporal variations in aerosol-liquid water cloud overlap and suggest that the frequency of occurrence of such overlap events is far from being negligible globally.

1 Introduction

Both aerosol direct and indirect effects are under intense research since the last few decades (refer comprehensive reviews by Carslaw et al., 2010; Lohmann and Feichter, 2005; Quaas et al., 2009; and references therein). Aerosols are shown to have multiple effects on clouds. The most recent report by the Intergovernmental Panel on Climate Change (IPCC) now recognizes more indirect aerosol effects compared to its previous assessments (IPCC, 2007). However, the uncertainty estimates of these aerosol-cloud interactions reflect our limited knowledge on them, although there have been considerable improvements from both observational and modeling perspectives (Stevens and Feingold, 2009). Many aspects are thought to contribute to the lack of assessment of direct and indirect effects, their relative importance, and their sensitivity to meteorology and large scale dynamics on a global scale. As a result, this field of research remains far from being matured. One good example is ongoing research on physical interpretation of the positive relationship between aerosol optical depth and cloud cover (Quaas et al., 2010; and references therein). These uncertainties challenge us so much so that we need to revisit and understand the basic definitions of aerosol and cloud (Koren et al., 2007, 2008).

In the context of simulating aerosol effects, it can be argued that the most complex situations are present in the atmosphere when aerosols overlap very bright water cloud tops (Brioude et al., 2009; Chand et al., 2008, 2009; Peters et al., 2009; Waquet et al., 2009). There are many reasons as to why the quantification of aerosol-cloud overlap characteristics is necessary. Few of them are listed below.

1. Whether aerosols exert a net positive or negative direct radiative forcing is, apart from optical properties, composition and size distribution, shown to be dependent

on underlying cloud cover (Chand et al., 2009). As the amount of overlap increases, the system is likely to exert a net warming effect in case of absorbing aerosols such as smoke.

2. Resolving uncertainties in aerosol cloud interactions (e.g. AOD-cloud cover relationship, cloud-lifetime effect, semi-direct effect) requires knowledge on how closely they are placed horizontally and vertically. This has a direct influence on various processes, for example, cloud-top entrainment, cloud processing of aerosols, humidification and swelling of aerosols in the vicinity of clouds etc.

3. It is necessary to investigate characteristics of overlapping events to assess biases in cloud property retrievals as they are observed to be sensitive to the overlying aerosol layers (Wilcox et al., 2009). This is especially required for datasets from the heritage sensors like, Along Track Scanning Radiometer (ATSR), Advanced Very High Resolution Radiometer (AVHRR) and Moderate Resolution Imaging Spectroradiometer (MODIS) that have climate monitoring capabilities where high accuracy retrievals are demanded

However, detecting aerosol-cloud overlap from the existing passive satellite sensors is extremely difficult and the quantification of overlap characteristics is not possible. One of the revolutionary advantages of Cloud-Aerosol Lidar with Orthogonal Polarization (CALIOP) sensor onboard NASA's Cloud-Aerosol Lidar and Infrared Pathfinder Satellite Observations (CALIPSO) satellite (Winker et al., 2009) is that it enables us to quantify overlapping cases and their characteristics. Although there are very few studies that investigate overlapping cases (e.g., Brioude et al., 2009; Chand et al., 2008, 2009; Peters et al., 2009; Waquet et al., 2009), a global assessment is still lacking.

In the present study, answers to the following three questions are sought.

1. How frequently distinct aerosol layers occur over low level water clouds seasonally and globally? Such frequency is expressed in the seasonal spatial maps.

2. How closely aerosol and water cloud layers are placed vertically during overlapping events? This is shown in the joint histograms of aerosol layer base height and cloud layer top height for six latitudinal bands.
3. How geometrically thick aerosol and thin cloud layers are in such overlapping cases? This is expressed in the joint histograms of aerosol and cloud geometrical thicknesses.

The next section provides a brief description of data used and its processing methodology followed by discussion of results. The last section concludes the paper.

2 CALIPSO-CALIOP data processing

We use the standard CALIPSO 5 km Aerosol and Cloud Layer Version 3 products (June 2006–May 2010) for analysis. These products, their theoretical basis algorithms and validations are described in the works by Hu et al. (2009), Liu et al. (2009), Omar et al. (2009), Vaughan et al. (2009), Winker et al. (2009), and Young and Vaughan (2009). For the present study, it is important that the cloud-aerosol discrimination is achieved as accurately and realistically as possible. We use quality flags provided in these datasets and use collocated observations only when both of these features are classified with highest confidence. The CALIPSO products are not entirely free from misclassifications, but nevertheless, they provide first such possibility to investigate aerosol-cloud overlap. For aerosols, most of the misclassifications are so far reported for cases when there are heavy outbreaks of dust over the desert areas. But as we will show later, overlap events are uncommon over these areas. As for the clouds, very thin clouds can occasionally be misclassified as aerosols. But such cases are also uncommon in the lower troposphere.

We analysed data separately for DJF (December–February), MAM (March, April and May), JJA (June–August), and SON (September, October and November) months to investigate seasonal variability in overlap characteristics. We further subdivide the globe into six latitude bands, i.e. 0–30° N, 30° N–60° N, 60° N–82° N, 0–30° S, 30° S–60° S, and 60° S–82° S. It is to be noted that observations polewards of 82° are not available from the CALIPSO due to its narrow swath and orbital configuration. The spatial sampling/coverage of the CALIOP is not as good as imagers, but we argue that the observations compiled over four seasons should be sufficient to draw robust conclusions.

For each collocated profile from the layered products, we first search for aerosol feature. If it is present, we examine its quality and proceed if it was detected with highest confidence. We then search if there is an underlying water cloud layer present in the same profile. If so, we examine its quality and proceed if it was also detected with highest confidence. We first search for aerosol layer and then an underlying cloud layer for computational efficiency reason as the number of cloud contaminated profiles is likely to be very high. We calculate the fraction of these cases for each 1°×1° grid box by dividing the number of these high confidence overlapping cases by the total number of observations over this grid box (averaged over four seasons). The use of only high quality observations would give conservative estimates of overlap frequency. We further compute joint histograms of aerosol base height and cloud top height. The advantage of presenting these histograms is that, apart from obtaining information on two important parameters (i.e. cloud top and aerosol base altitudes), we can also relate how closely they are present in the atmosphere. Closer the distribution centered along the diagonal axis of a joint histogram, minimum is the vertical distance between aerosol and cloud layers. We investigate joint histograms of geometrical thicknesses of aerosols and cloud layers as they also play a substantial role in radiative transfer.

One of the many distinguishing abilities of CALIOP observations is their ability to classify aerosols into various categories (Omar et al., 2009). The standard 5 km Aerosol Layer data product provides classification of aerosols into six types, namely, clean marine, dust, polluted continental, clean continental, polluted dust, and smoke by making use of layer integrated attenuated backscatter and volume depolarization ratio (along with ancillary information on the surface type and layer height) and following a sound physical basis (Omar et al., 2009). While making use of such categorization, we compute overlap frequency also for smoke layers separately.

3 Results on overlap statistics

First, it is helpful to examine the climatological distribution of low level liquid water clouds and aerosols globally in order to get an overview of regions where overlapping situations are most likely to occur. Since the large scale circulations would have a first order impact on the transport of aerosols over the oceans, it is necessary to discuss major wind patterns in this context. Figure 1 shows the climatological distribution of daytime low level liquid clouds and their seasonality based on the International Satellite Cloud Climatology Project (ISCCP) D2 data (1983–2008). It can be seen that oceanic areas where upwelling of cold water takes place along the western coasts of the continents show predominance of these clouds. For example, the parts of western coasts of North and South American continents as well as southwestern coast of Africa show very high frequency of these clouds. Another region that stands out is the belt of low level cloudiness between latitudes 30° S–60° S in the Southern Ocean. Globally, the fraction of low level clouds is highest during JJA months. A global view of aerosols (Fig. 2 and Remer et al., 2008) shows that there are many regions where aerosol-cloud overlaps are likely to occur as both natural and anthropogenic aerosols are transported over oceanic areas where low level liquid clouds are present in high amounts. For example, easterly and southeasterly winds (Supplementary Figs. S1 and S2) transport biomass burning aerosols from Southern Africa over to Southeast Atlantic Ocean, while westerly winds carry biomass burning and other aerosols over Northern Pacific Ocean from Siberia and the Northeast Asian regions. The Supplementary Fig. S3 shows the typical global spatial distribution of burning events and their seasonality in terms of 10-day composite fire maps derived from the MODIS sensor for year 2008 to further facilitate interpretation of the results below.

The spatial patterns of overlap frequency and their seasonal variations, shown in Figs. 3 and 4, precisely capture these overlap events. All aerosol types are considered for the results shown in Fig. 3 (hereafter denoted as all-aerosol-overlap, AAO, case), while the results for only smoke aerosols are shown in Fig. 4 (smoke-aerosol-overlap, SAO, cases). A distinct seasonality in overlap frequency is evident in both cases (Figs. 3 and 4). The frequency is highest during JJA months in AAO case, while in SAO case, it is highest in SON months.

In DJF months, the maximum frequency is observed off the western coast of Central Africa with values occasionally exceeding 15% for AAO case. Based on the spatial distributions of low clouds and aerosols together with major circulation patterns, it can be deduced that easterly and northeasterly winds over arid as well as intense biomass burning regions of tropical savannas in sub-Saharan Africa transport dust and smoke aerosols south of the equator. The Multiangle Imaging Spectroradiometer (MISR) aerosol optical depth shows maximum values off the southern coast of Liberia, Ivory Coast, Ghana and Nigeria in DJF months (Fig. 2). Aerosols from the regions of Southwestern Africa are also transported above these clouds. Another region that shows high overlap frequency is China.

The transport of biomass burning and dust aerosols from the Eurasia region intensifies in MAM months. The westerly winds advect these aerosols over Northern Pacific Ocean off the eastern coasts of China, Russia and Japan, where low level clouds are also present in high amounts, resulting in high overlap frequency over this region (>15%). The overlap frequency off western coast of sub-Saharan Africa is high in AAO case, which may be due to the transport of pure and polluted dust as it is not seen in SAO case. During JJA months, oceanic areas along the eastern and western coasts of the African continent show high overlap frequency with mean values exceeding 20%. Strong monsoonal winds (Somali jet) lift and transport large quantities of dust aerosols from East African regions over Northern Indian Ocean and Arabian Sea, where shallow as well as deep convection is observed during monsoon months. The overlap due to smoke aerosols is observed off the western coast of Southern Africa, where biomass burning is intensified during this season. The MISR AOD composites also show high values over Southeast Atlantic Ocean and Southern Africa. The overlap frequency is also very high off western coasts of South America (Columbia, Ecuador, and Peru), and North America (California, USA, and Western Mexican coast). During SON months, aerosol transport from biomass burning regions of Southern and Central Africa as well as South America dominates the global distribution of overlap frequency.

In addition to overlap frequency, the vertical separation of aerosol and cloud layers and their geometrical thickness have an impact on radiative transfer by influencing multiple reflection and absorption processes locally. The altitudes at which these interactions occur play an important role in shaping radiative heating profiles during overlap events. Therefore, in order to gain information on the vertical distribution, observations of cloud layer top and aerosol layer base altitudes, and their geometrical thicknesses are expressed in terms of joint histograms as shown in Figs. 5 and 6 for the AAO case. The histograms are computed for six latitude bands (60° N–90° N, 30° N–60° N, 0°–30° N, 0°–30° S, 30° S–60° S, and 60° S–90° S) and for four seasons. It can be seen from Fig. 5 that, in bulk of overlapping events, cloud layer top and aerosol layer base altitudes are within the lowermost 3 km of the troposphere. In the tropical regions, aerosol layer bases are 2–3 km high in 30–35% cases, and altogether in more than 50% cases they are within 2–4 km (Fig. 7a). About 45–50% aerosol layers have their bases within 1–3 km in the polar regions. In almost all latitudinal bands, the bulk of cloud layers have their tops within 1–2 km (about 60% in 0°–30° S to about 45% in the polar regions).

There is a clear tendency that the vertical separation between aerosol and cloud layers increases from high to low latitude regions in both hemispheres. In the polar regions, the maximum in frequency distribution is aligned diagonally in joint histograms suggesting that, in most cases, aerosol and cloud layers are spaced very close to each other, while at lower latitudes, maxima in the distributions have a large scatter diagonally. The spatio-temporal variability of aerosol sources together with the large scale atmospheric circulation patterns are mostly responsible for such a hemispheric tendency in the vertical separation of aerosol and cloud layers. For example, in the tropical bands where a large scatter in joint histograms is observed, dust and biomass burning aerosols are convected/injected to higher altitudes and then transported over the nearby regions where low level clouds are present. In the polar regions, the large scale subsidence and strong and persistent inversions (Devasthale et al., 2010) lead to very high stability. Figure 7c shows the cumulative frequency of the vertical distance between aerosol and cloud layers. In general, in about 5–10% cases the vertical distance between aerosol and cloud layers is less than 100 m, while about in 45–60% cases it less than a kilometer in the annual means for different latitudinal bands.

The Fig. 5 also depicts seasonal variability in the aerosol and cloud layer separation for various latitude bands. The intra-annual variability also increases from high to low latitudes. The latitude band of 0°–30° S exhibits the highest seasonal variability mostly driven by seasonalilty in the biomass burning events over the sub-Saharan and Central African regions. Aerosols injected at high altitudes over the biomass burning regions in South America, which are then advected over the Eastern Pacific Ocean across the Andes by easterly and southeasterly winds, also contribute to this observed variability. In general, while cloud layer tops are mostly below 2 km, the bulk of aerosol layers can remain as high as 4 km. The northern hemispheric latitude band (i.e. 0°–30° N) also shows high seasonal variability due to seasonality in the pure and polluted dust aerosols. The largest vertical separation between aerosol and cloud layers is observed over the 0°–30° S latitude band and for SON months.

The majority of aerosol and cloud layers have geometrical thicknesses less than a kilometer during overlap events (Figs. 6 and 7d). In most cases, cloud layers are thicker than aerosol layers over all latitude bands and seasons, but the frequency of occurrence of thicker aerosol layers gradually increases from poles to tropics. The distributions of aerosol layer thickness are narrow over polar regions, while they are much broader over the tropical regions. Aerosol layers can be occasionally as thick as 4 km over the tropical regions. In about 70–80% cases, aerosol layers are less than a kilometer thick, while in about 18–22% cases they are 1–2 km thick. The frequency of aerosol layers 2–3 km thick is about 4–5% in the tropical belts during overlap events.

4 Conclusions and implications

We present, for the first time, a global overview of aerosol-liquid water cloud overlap using four years of collocated CALIPSO 5 km Aerosol and Cloud V3 Layer products (June 2006–May 2010). The presence of aerosols over highly reflective surfaces, such as bright water cloud tops, could significantly alter their net radiative effect. A quantitative assessment of aerosol-cloud overlap is necessary to fully understand aerosol direct and indirect effects, and to estimate the uncertainties in cloud property retrievals from passive remote sensing instruments. The capability of CALIPSO to vertically resolve overlapping cases is exploited in the present study to understand the frequency of such overlaps and their global seasonal distribution. The characteristics of overlap events are examined in terms of joint histograms of cloud layer top altitude and aerosol layer base altitude, and cloud and aerosol layer geometrical thicknesses in overlapping events.

The results show a distinct seasonality in overlap frequency in both AAO (all aerosols) and SAO (smoke aerosols) cases. Globally, the frequency is highest during JJA months in AAO case, which is most likely due to the dominance of dust and smoke aerosols over low level water clouds. While for the SAO case, it is highest in SON months due to the dominance of smoke from biomass burning. The seasonal mean overlap frequency can regionally exceed 20% in AAO case and 10% in SAO case. There is a tendency that the vertical separation between aerosol and cloud layers increases from high to low latitude regions in the both hemispheres. In about 5–10% cases the vertical distance between aerosol and cloud layers is less than 100 m, while about in 45–60% cases it less than a kilometer in the annual means for different latitudinal bands. The frequency of occurrence of thicker aerosol layers gradually increases from poles to tropics. In about 70–80% cases, aerosol layers are less than a kilometer thick, while in about 18–22% cases they are 1–2 km thick. The frequency of aerosol layers 2–3 km thick is about 4–5% in the tropical belts during overlap events.

The results from our study imply that the frequency of occurrence of aerosol-water cloud overlaps is far from negligible. There should be more emphasis on observational and modeling studies in this direction to fully quantify radiative impact of observed overlap globally and regionally. For example, by applying constraints from CALIPSO data, the studies like Chand et al. (2009), Peters et al. (2009) and Podgorny and Ramanathan (2001) could be further extended on a global scale. It is also necessary to understand differences in the net radiative impact of overlap events over the polar and tropical regions as they exhibit different meteorological regimes. Here, it is observed that, in bulk of overlap events, aerosol and cloud layers are placed vertically very close. Even after allowing for the misclassification of the precise boundaries between the two, this small vertical separation would mean that there is a high likelihood that aerosol-cloud interactions are manifested in overlap events. However, it remains to be evaluated in which dominant form and at what magnitude these manifestations occur globally. It is to be noted that the regions where overlap frequency is high, aerosol optical depths are also often large (e.g., optically thick plumes of dust and smoke). Therefore, critical evaluations of accuracy of cloud property retrievals from the heritage sensors (ATSR, AVHRR, and MODIS) are needed over overlap regions if these retrievals are to be used for climate applications.

We have shown that the CALIPSO-CALIOP data are extremely useful in characterizing these otherwise highly complex overlap situations, and these data should provide rigorous constraints on modeling the net radiative impact of aerosol-liquid water cloud overlaps globally. The present study focuses on characterizing macrophyiscal properties of overlapping events, thus only partially exploiting the full capability of CALIPSO-CALIOP observations.

Supplementary material related to this article is available online at: http://www.atmos-chem-phys-discuss.net/10/22109/2010/ acpd-10-22109-2010-supplement.pdf.

Acknowledgements. Authors are grateful to the CALIPSO Science Team for their efforts in making data products publicly available. These data were obtained from the NASA Langley Research Center Atmospheric Science Data Center. Authors are also thankful to ISCCP, NASA's GIOVANNI and MODIS Rapid Response System projects for making cloud, aerosol and fire map datasets available for research. Wind data were obtained from the ECMWF's ERA-Interim project. This work was supported by the Swedish National Space Board.

References

Brioude, J., Cooper, O. R., Feingold, G., Trainer, M., Freitas, S. R., Kowal, D., Ayers, J. K., Prins, E., Minnis, P., McKeen, S. A., Frost, G. J., and Hsie, E.-Y.: Effect of biomass burning on marine stratocumulus clouds off the California coast, Atmos. Chem. Phys., 9, 8841–8856, doi:10.5194/acp-9-8841-2009, 2009.

Carslaw, K. S., Boucher, O., Spracklen, D. V., Mann, G. W., Rae, J. G. L., Woodward, S., and Kulmala, M.: A review of natural aerosol interactions and feedbacks within the Earth system, Atmos. Chem. Phys., 10, 1701–1737, doi:10.5194/acp-10-1701-2010, 2010.

Chand, D., Anderson, T. L., Wood, R., Charlson, R. J., Hu, Y., Liu, Z., and Vaughan, M.: Quantifying above-cloud aerosol using spaceborne lidar for improved understanding of cloudy-sky direct climate forcing, J. Geophys. Res., 113, D13206, doi:10.1029/2007JD009433, 2008.

Chand, D., Wood, R., Anderson, T. L., Satheesh, S. K., and Charlson, R. J.: Satellite-derived direct radiative effect of aerosols dependent on cloud cover, Nat. Geosci., 2, 181–184, doi:10.1038/NGEO437, 2009.

Devasthale, A., Willén, U., Karlsson, K.-G., and Jones, C. G.: Quantifying the clear-sky temperature inversion frequency and strength over the Arctic Ocean during summer and winter seasons from AIRS profiles, Atmos. Chem. Phys., 10, 5565–5572, doi:10.5194/acp-10-5565-2010, 2010.

Hu, Y., Winker, D., Vaughan, M., Lin, B., Omar, A., Trepte, C., Flittner, D., Yang, P., Nasiri, S. L., Baum, B., Sun, W., Liu, Z., Wang, Z., Young, S., Stamnes, K., Huang, J., Kuehn, R., and Holz, R.: CALIPSO/CALIOP cloud phase discrimination algorithm, J. Atmos. Ocean. Tech., 26, 2293–2309. 2009.

Intergovernmental Panel of Climate Change (IPCC): The Physical Science Basis, Contribution of Working Group I to the Fourth Assessment Report of the IPCC 916, Cambridge Univ. Press, Cambridge, United Kingdom and New York, NY, USA, 2007.

Koren, I., Oreopoulos, L., Feingold, G., Remer, L. A., and Altaratz, O.: How small is a small cloud?, Atmos. Chem. Phys., 8, 3855–3864, doi:10.5194/acp-8-3855-2008, 2008.

Koren, I., Remer, L. A., Kaufman, Y. J., Rudich, Y., and Martins, J. V.: On the twilight zone between clouds and aerosols, Geophys. Res. Lett., 34, L08805, doi:10.1029/2007GL029253, 2007.

Liu, Z., Vaughan, M. A., Winker, D. M., Kittaka, C., Kuehn, R. E., Getzewich, B. J., Trepte, C. R., and Hostetler, C. A.: The CALIPSO lidar cloud and aerosol discrimination: version 2 algorithm and initial assessment of performance, J. Atmos. Ocean. Tech., 26, 1198–1213, doi:10.1175/2009JTECHA1229.1, 2009.

Lohmann, U. and Feichter, J.: Global indirect aerosol effects: a review, Atmos. Chem. Phys., 5, 715–737, doi:10.5194/acp-5-715-2005, 2005.

Omar, A., Winker, D., Kittaka, C., Vaughan, M., Liu, Z., Hu, Y., Trepte, C., Rogers, R., Ferrare, R., Kuehn, R., and Hostetler, C.: The CALIPSO automated aerosol classification and lidar ratio selection algorithm, J. Atmos. Ocean. Tech., 26, 1994–2014, doi:10.1175/2009-JTECHA1231.1, 2009.

Peters, K., Quaas, J., and Bellouin, N.: Effects of absorbing aerosols in cloudy skies: a satellite study over the Atlantic Ocean, Atmos. Chem. Phys. Discuss., 9, 20853–20880, doi:10.5194/acpd-9-20853-2009, 2009.

Podgorny, I. A. and Ramanathan, V.: A modeling study of the direct effect of aerosols over the tropical Indian Ocean, J. Geophys. Res., 106, 24097–24105, 2001.

Quaas, J., Ming, Y., Menon, S., Takemura, T., Wang, M., Penner, J. E., Gettelman, A., Lohmann, U., Bellouin, N., Boucher, O., Sayer, A. M., Thomas, G. E., McComiskey, A., Feingold, G., Hoose, C., Kristjnsson, J. E., Liu, X., Balkanski, Y., Donner, L. J., Ginoux, P. A., Stier, P., Grandey, B., Feichter, J., Sednev, I., Bauer, S. E., Koch, D., Grainger, R. G., Kirkevåg, A., Iversen, T., Seland, Ø., Easter, R., Ghan, S. J., Rasch, P. J., Morrison, H., Lamarque, J.-F., Iacono, M. J., Kinne, S., and Schulz, M.: Aerosol indirect effects – general circulation model intercomparison and evaluation with satellite data, Atmos. Chem. Phys., 9, 8697–8717, doi:10.5194/acp-9-8697-2009, 2009a.

Quaas, J., Stevens, B., Stier, P., and Lohmann, U.: Interpreting the cloud cover – aerosol optical depth relationship found in satellite data using a general circulation model, Atmos. Chem. Phys., 10, 6129–6135, doi:10.5194/acp-10-6129-2010, 2010.

ACPD
10, 22109–22130, 2010

A global survey of aerosol-liquid water cloud overlap

A. Devasthale and
M. A. Thomas

Title Page
Abstract | Introduction
Conclusions | References
Tables | Figures
◀| |▶
◀ ▶
Back | Close
Full Screen / Esc
Printer-friendly Version
Interactive Discussion

Remer, L. A., Kleidman, R. G., Levy, R. C., et al.: Global aerosol climatology from the MODIS satellite sensors, J. Geophys. Res., 113, D14S07, doi:10.1029/2007JD009661, 2008.

Stevens, B. and Feingold, G.: Untangling aerosol effects on clouds and precipitation in a buffered system, Nature, 461, 607–613, 2009.

Vaughan, M., Powell, K., Kuehn, R., Young, S., Winker, D., Hostetler, C., Hunt, W., Liu, Z., McGill, M., and Getzewich, B.: Fully automated detection of cloud and aerosol layers in the CALIPSO lidar measurements, J. Atmos. Ocean. Tech., 26, 2034–2050, doi:10.1175/2009JTECHA1228.1, 2009.

Waquet, F., Riedi, J., Labonnote, L. C., and Goloub, P., Cairns, B., Deuze, J.-L., and Tanre, D.: Aerosol remote sensing over clouds using A-train observations, J. Atmos. Sci., 66, 2468–2480, 2009.

Wilcox, E. M., Harshvardhan, and Platnick, S.: Estimate of the impact of absorbing aerosol over cloud on the MODIS retrievals of cloud optical thickness and effective radius using two independent retrievals of liquid water path, J. Geophys. Res., 114, D05210, doi:10.1029/2008JD010589, 2009.

Winker, D. M., Vaughan, M. A., Omar, A. H., Hu, Y., Powell, K. A., Liu, Z., Hunt, W. H., and Young, S. A.: Overview of the CALIPSO Mission and CALIOP data processing algorithms, J. Atmos. Ocean. Tech., 26, 2310–2323, doi:10.1175/2009JTECHA1281.1, 2009.

Young, S. A. and Vaughan, M. A.: The retrieval of profiles of particulate extinction from Cloud Aerosol Lidar Infrared Pathfinder Satellite Observations (CALIPSO) data: algorithm description, J. Atmos. Ocean. Tech., 26, 1105–1119, doi:10.1175/2008 JTECHA1221.1, 2009.

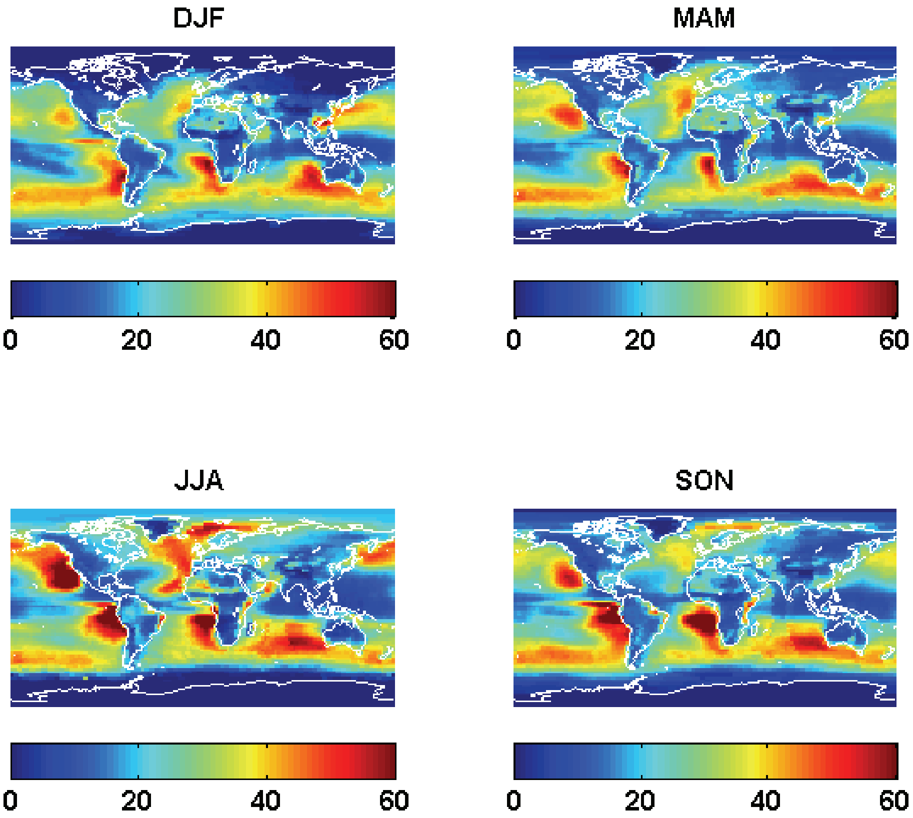

Fig. 1. A global climatological distribution (1983–2008) of daytime low level liquid water clouds derived from ISCCP D2 product for DJF, MAM, JJA, and SON months. These data were obtained from the ISCCP website: http://isccp.giss.nasa.gov/products/browsed2.html.

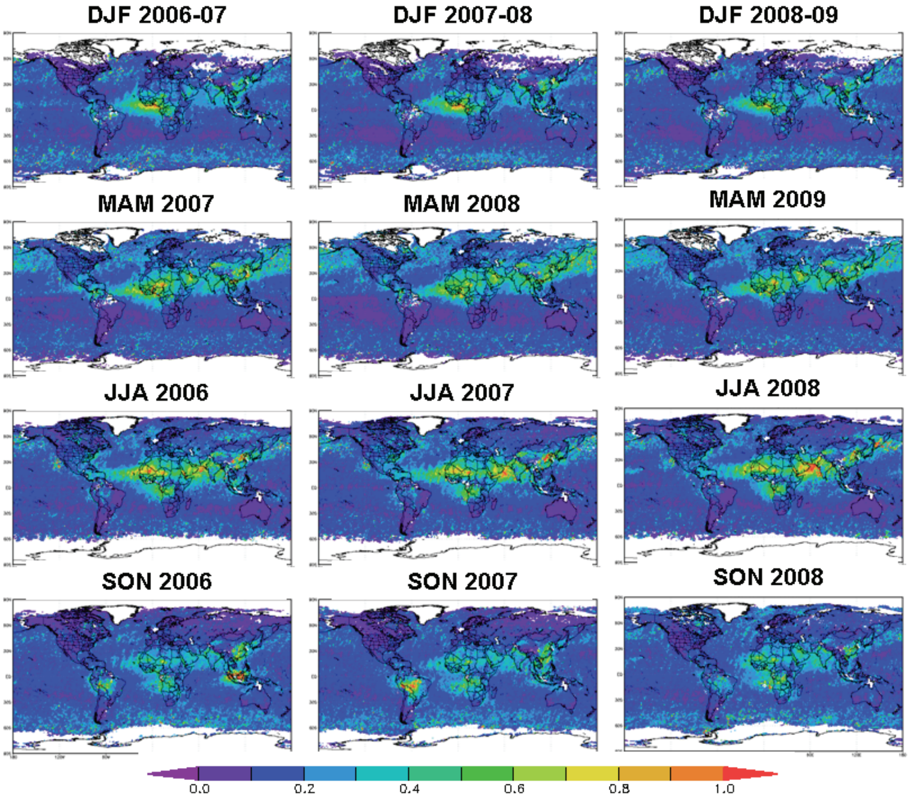

Fig. 2. Mean seasonal aerosol optical depths derived from the MISR sensor.

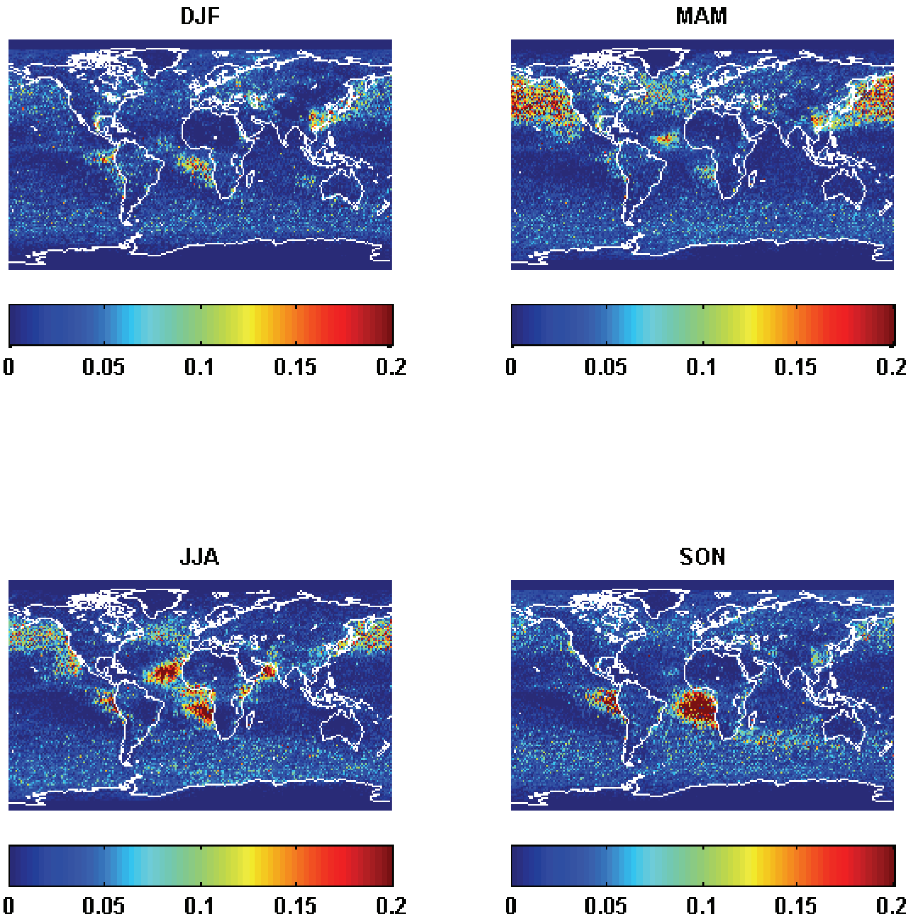

Fig. 3. The spatial and seasonal aerosol-water cloud overlap frequency when all aerosol types are considered for the analysis.

Title Page
Abstract | Introduction
Conclusions | References
Tables | Figures
◀| |▶
◀ ▶
Back | Close
Full Screen / Esc
Printer-friendly Version
Interactive Discussion

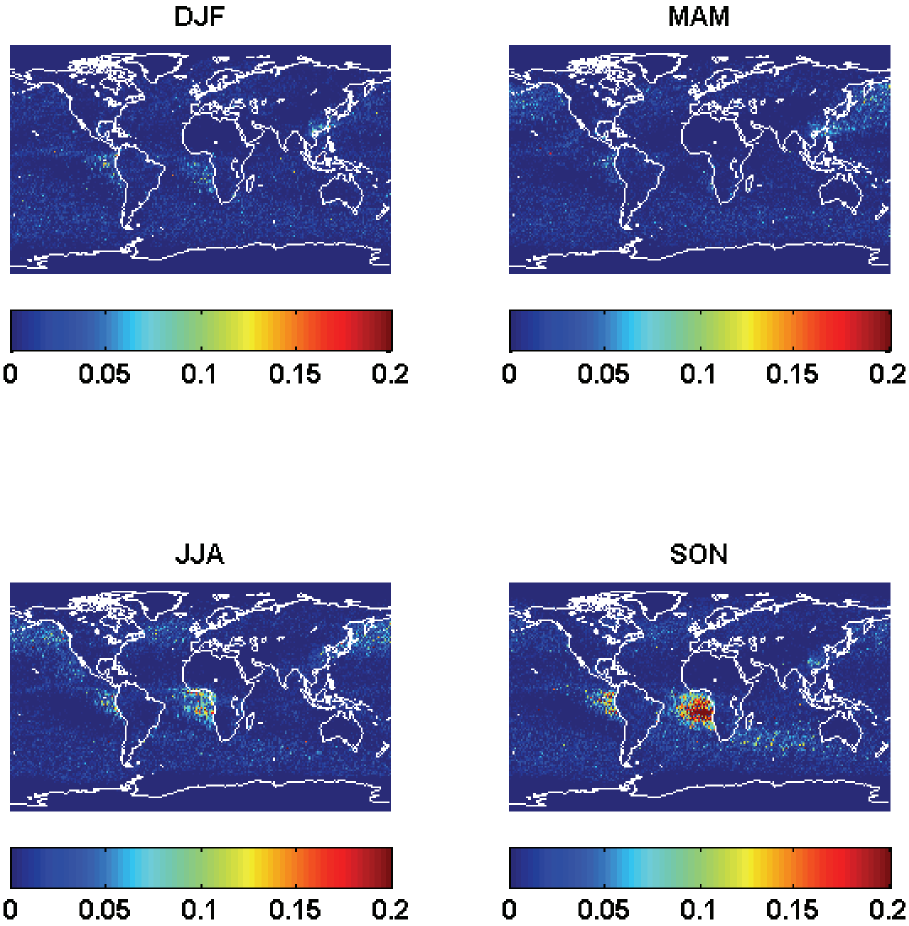

Fig. 4. Same is in Fig. 3, but for cases when only smoke layers are included in the analysis.

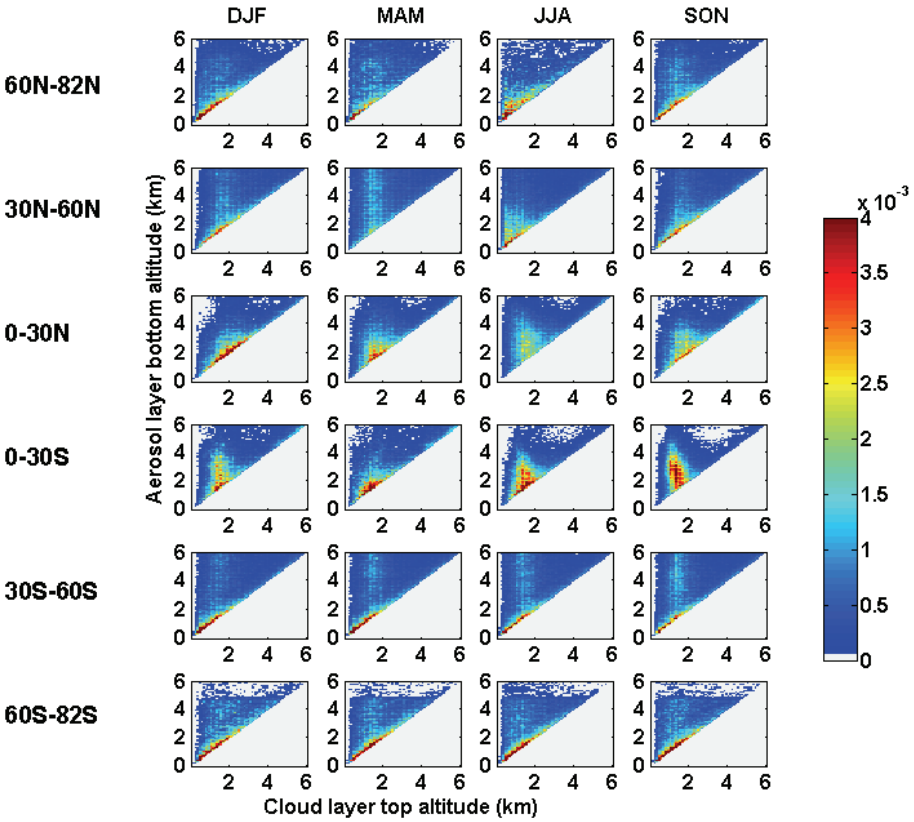

Fig. 5. The joint histograms of cloud layer top altitude and aerosol layer base altitude in overlapping cases when overlap from all aerosol types is considered. The bin size is 100 m by 100 m and the observations in each height-height bin are normalized by the total number of observations in the entire histogram.

Title Page
Abstract | Introduction
Conclusions | References
Tables | Figures
◀| |▶
◀ ▶
Back | Close
Full Screen / Esc
Printer-friendly Version
Interactive Discussion

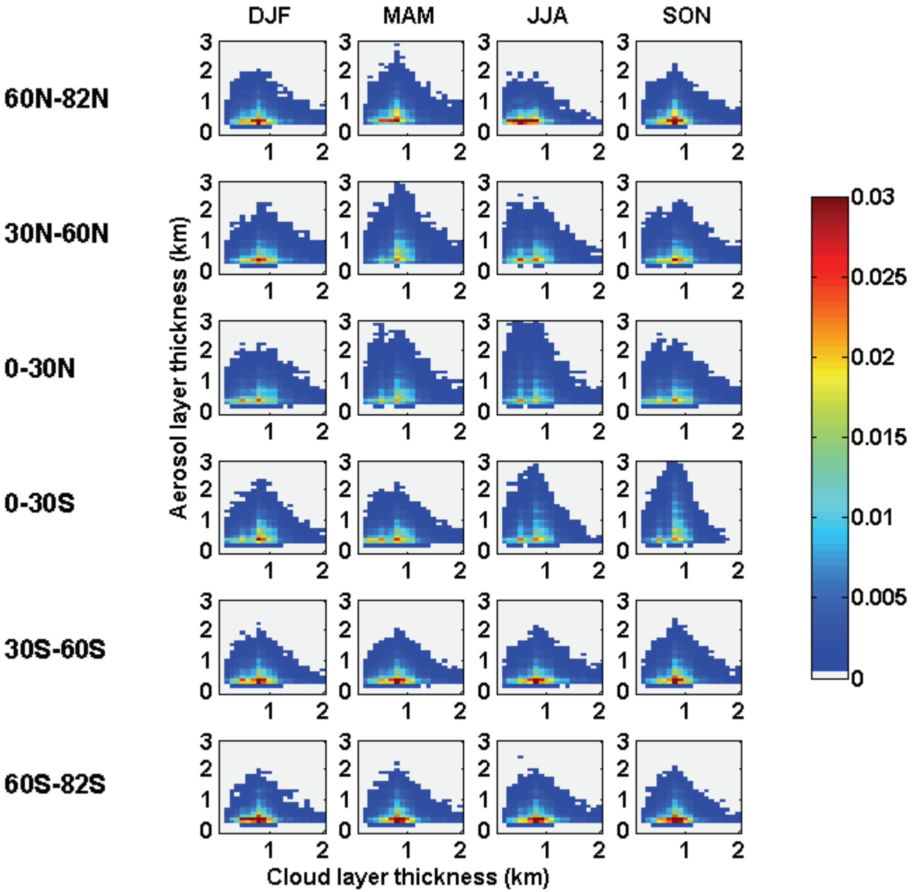

Fig. 6. Joint histograms of cloud and aerosol layer geometrical thicknesses in overlapping cases when overlap from all aerosol types is considered. The binning and normalization is same as in Fig. 5.

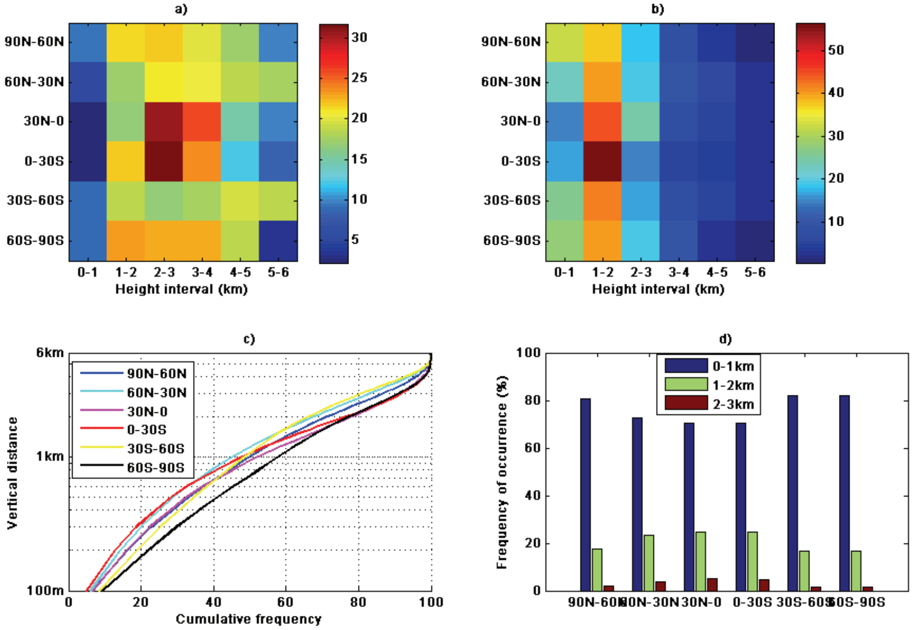

Fig. 7. Annual mean **(a)** frequency of occurrence of aerosol layer base altitudes; **(b)** frequency of occurrence of cloud layer top altitudes; **(c)** cumulative frequency of the vertical distance between aerosol and cloud layers; and **(d)** frequency of occurrence of aerosol layer geometrical thickness in the intervals of 0–1 km, 1–2 km and 2–3 km. Note that all of these statistics are computed only for cases when overlap was observed.

Title Page
Abstract
Introduction
Conclusions
References
Tables
Figures
◀
▶
Back
Close
Full Screen / Esc
Printer-friendly Version
Interactive Discussion